J. Phys. D: Appl. Phys. **19** (1986) 1311–1320. Printed in Great Britain

Surface and bulk magnetic behaviour of sputtered CoCr films

K Hemmes†, W Lisowski‡, J C Lodder†, L J Hanekamp† and Th J A Popma†

† Twente University of Technology, PO Box 217, 7500 AE Enschede, The Netherlands

‡ Institute of Physical Chemistry, Polish Academy of Sciences, Kasprazaka 44/52, 01-224 Warszawa, Poland

Received 11 October 1985

Abstract. The magnetic hysteresis curve at the surface of RF- and magnetron-sputtered CoCr (81/19 at.%), in the thickness range of 20–2500 nm, was measured with a rotating-analyser apparatus using the magneto-optic Kerr effect. The Kerr rotation of CoCr films (13–19 at.% Cr) decreases with increasing Cr content, and depends slightly on wavelength, showing a faint minimum between 550 and 600 nm. The surface hysteresis is compared with the bulk hysteresis as measured with a VSM. For RF films the maximum surface coercivity is higher than the bulk coercivity, being 120 and 95 kA m^{-1} respectively for 80 nm thick films but an abrupt decrease in only the surface coercivity was found at $t = 125$ nm. The coercivity of magnetron-sputtered CoCr deviates from that of RF-sputtered films. Until a maximum coercivity is reached at $\simeq 1$ μm, the surface coercivity is about 20% higher, but at $\simeq 2$ μm both coercivities decrease strongly. The existence of reversed domains within the main domains of CoCr is proposed, and the reversal mechanism is thought to be one in which the reversed domains grow at the expense of the main domain.

1. Introduction

CoCr thin films are a suitable medium for perpendicular magnetic recording (Iwasaki 1980). It is well known that the magnetic properties of sputtered CoCr layers are strongly related to the preparation conditions. The coercivity H_c is one of the most relevant parameters in recording. Therefore we have studied H_c as a function of two different deposition methods namely RF and magnetron sputtering. We also compared the bulk coercivity as measured with a vibrating-sample magnetometer (VSM) with the surface coercivity obtained from magneto-optic polar Kerr measurements. Abe *et al* (1982) found that the Kerr coercivity of 1 μm thick RF-sputtered CoCr (21.5 at.% Cr) is lower than the coercivity measured by a VSM. The opposite was found for magnetron films of 0.3 μm thickness in the composition range of 11 to 28 at.% (Tsutsumi *et al* 1983). The most recent study by Smits *et al* (1984) reports on RF-sputtered CoCr (21.5 at.% Cr) in the range of 30–900 nm on Si and polyimide substrates. They found a critical thickness of $\simeq$400 nm below which the Kerr coercivity is higher and above which it is lower than the VSM coercivity. The very thinnest films form an exception since both coercivities are about the same here.

Our results confirm the existence of a critical thickness in RF-sputtered CoCr films (at 125 nm), consistent with the work of Abe and Smits and co-workers. The deviating

behaviour of magnetron films as observed by Tsutsumi and co-workers is also confirmed in this study.

2. Sample preparation

All CoCr samples were sputtered in a Leybold–Heraeus RF-sputter apparatus either with or without magnetron facilities. We shall distinguish here between RF- and magnetron-sputtered CoCr films. In RF sputtering four Si(100) substrates of 1 × 1 cm were placed in the centre of the substrate holder and in magnetron sputtering either 5, 7 or 13 Si substrates were placed on the holder. RF samples were sputtered from an alloyed CoCr 81/19 at.% target under the following optimised conditions, determined for the same apparatus by Lodder and Wielinga (1984); $V_{rf} = -1.6$ kV and $P_{ar} = 0.4$ Pa, and in magnetron sputtering (also from an alloyed CoCr 81/19 at.% target) $V_{rf} = -250$ V and $P_{ar} = 0.6$ Pa. Also 13 and 15 at.% Cr films were RF sputtered under the same conditions from an alloyed and a composite target respectively. The composition was checked with x-ray fluorescence.

3. Magneto-optic Kerr rotation apparatus

A rotating-analyser ellipsometer (Hanekamp *et al* 1982) was applied in order to measure the polar Kerr rotation. The samples were placed perpendicular to the magnetic field between the poles of an electromagnet. The light was coupled in and out by means of a small mirror cut from a Si wafer coated with Al and placed at an angle of 45° with the sample. As an alternative to the Kerr enhancement by means of a dielectric layer, a multiple-reflection holder was developed with which up to four reflections on the sample could be obtained, thus increasing the Kerr rotation by a factor of four (see figure 1).

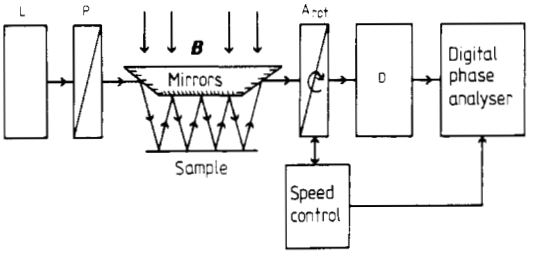

Figure 1. Schematic diagram of the rotating analyser apparatus with a multiple-reflection sample holder, showing rotating analyser(A_{rot}), detector (D), light source (L), and polariser (P).

The limiting factors in obtaining more reflections are the size of the sample and the mirrors, and the diameter of the light beam. Neglecting the ellipticity the intensity on the detector at a time τ is given by

$$I = I_0 \cos^2(\omega\tau - \theta(H)) = I_0[1 + \cos(2\omega\tau - 2\theta(H))]/2$$

ω being the angular velocity of the analyser and $\theta(H)$ the field-dependent angle between

the polarisation direction of the light before and after reflection from the sample. The phase difference of the detected signal compared with a reference signal obtained from the rotating analyser is determined. Only the field dependence of this phase is important here and yields the Kerr rotation with a factor of two, which is one of the most important advantages of this method. Therefore the measured phase difference between the up and down saturation magnetisation with four reflections is 16 times the single Kerr rotation. However in most measurements two reflections are used in order to save time in aligning the system and because the accuracy with two reflections is high enough to determine the coercive force within 4 kA m^{-1} (50 Oe). Drift in the offset value is a more important cause of inaccuracy. The drift was checked by measuring the remnant value at zero field after magnetic saturation ($+M_s$) just before and after each measurement. Occasionally a drift of 0.05 deg was tolerated and could be corrected for without introducing too large an error, but in most cases the drift was smaller than 0.02 deg in the displayed phase difference. In a two-reflection measurement this means a drift of only 0.005 deg compared with the single Kerr rotation. The accuracy of the Kerr measurements is indicated in the figures where the Kerr/VSM coercivity ratio is plotted and in the hysteresis curves.

The wavelength dependence of the Kerr rotation was measured by using a halogen lamp and a monochromator. In this set-up a photomultiplier detector and the 'one-reflection sample holder' were used. All hysteresis curves were measured using light with a wavelength of 632 nm, either from a HeNe laser or from the monochromator, with beam diameters of 1 and 3 mm respectively.

4. Experimental results

4.1. Wavelength dependence

The wavelength dependence of the Kerr rotation for different alloy compositions of CoCr (13, 15 and 19 at.% Cr) was measured in the region of 350–1000 nm. All compositions exhibit the same functional dependence on wavelength with a faint minimum at 550–600 nm. A tendency can be observed for the minimum to shift to longer wavelengths with higher Cr content (see figure 2). For the 13 at.% Cr sample saturation was not completely achieved at 10 kOe. VSM measurements indicate that saturation is only reached at ≈14 kOe. Therefore those values in figure 2 should be about 30% higher. Abe *et al* (1982) found a minimum of 0.063 deg at 560 nm for a 21.5 at.% Cr alloy in agreement with a decreasing θ_K (and M_s) with increasing Cr content, also reported by Tsutsumi *et al* (1983). The lower values of the Kerr rotation for the magnetron sample in figure 2 were not systematically measured, but are indicative of the spread in θ_K over different samples. For both the RF and magnetron series the average Kerr rotation at 632 nm is 0.10 deg with a standard deviation of less than 0.01 deg. The Kerr rotation of the RF samples tended to decrease slightly with increasing film thickness, whereas for magnetron films no correlation with film thickness was found.

4.2. A comparison between surface and bulk properties

The magnetisation measured with a VSM is the average magnetisation of the whole sample, while the magneto-optic Kerr rotation is only determined by the magnetisation of the surface layer, whose thickness is equal to the penetration depth of light (≈15 nm for CoCr in the visible region). Therefore, the difference between the two measurements

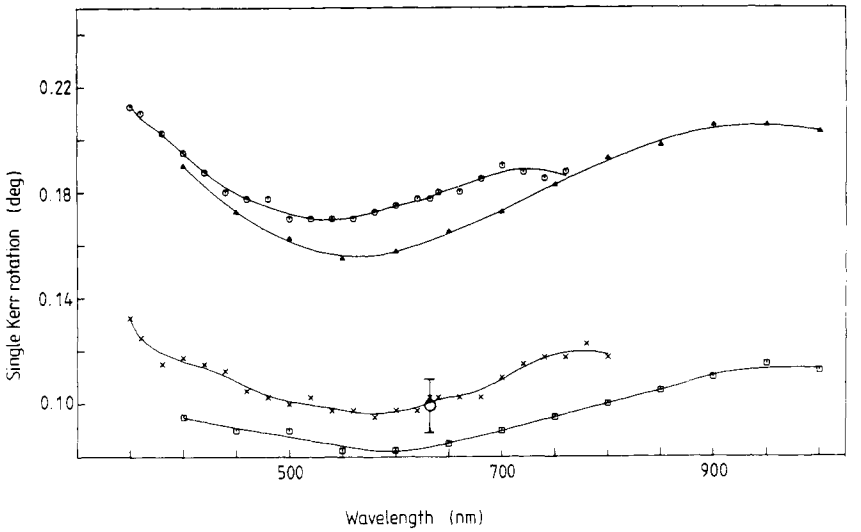

Figure 2. Wavelength dependence of the single polar Kerr rotation θ_K for three alloy compositions of CoCr: ⊙, 87/13 at.%; △, 85/15 at.%; ×, 81/19 at.% and □, 81/19 at.% magnetron. The average θ_K plus standard deviation of all 19 at.% samples is plotted as a circle with error bars at 633 nm.

is proof of a non-uniform magnetisation throughout the film. Although hysteresis curves were measured for all samples, we will concentrate here on the coercivity.

In studying the coercivity of sputtered CoCr films one is faced with a large intrinsic spread in the results although the external parameters are controlled as well as possible. Even for films in the same sputter run lying next to each other the spread can be large. To tackle this problem a large number of samples were measured. In RF sputtering 14 runs of four samples were sputtered to cover the thickness range t = 20–1000 nm. The total magnetic moment (M_s × volume) was determined by using a VSM calibrated with a pure Ni sample.

The saturation magnetisation M_s for both the RF and magnetron samples was determined at 460 kA m^{-1} from this moment combined with x-ray fluorescence and from earlier experiments (Lodder *et al* 1983, Hemmes *et al* 1984). Using M_s = 460 kA m^{-1} the (magnetic) film thickness (t) was calculated and plotted on a logarithmic scale along the x axis in the figures. In determining the VSM coercivity the curves for the thinnest films had first to be corrected for the diamagnetism of the sample holder.

4.2.1. RF-sputtered CoCr 81/19 at.%. The VSM coercivity of the RF-sputtered films as a function of film thickness exhibits a maximum of ≃95 kA m^{-1} (1200 Oe) at t = 80 nm (±20) and then slowly decreases with increasing thickness (see figure 3(*a*)). This is in agreement with earlier results under the same sputter conditions (Wielinga *et al* 1982). The surface or Kerr coercivity exhibits a higher maximum of 120 kA m^{-1} (1500 Oe) between 60 and 90 nm, but falls off almost discontinuously at t = 125 nm (±15). This is also reflected in figure 3(*b*) where the ratio of the surface and bulk coercivity is plotted as a function of the film thickness. By calculating this ratio the intrinsic spread per sample is cancelled out. The discontinuity at t = 125 nm is now clearly revealed. In the case of thicker films the Kerr coercivity is always smaller than the VSM value, whereas for thinner films the Kerr coercivity as a whole is larger. Only for the thinnest films (≃20 nm) is the

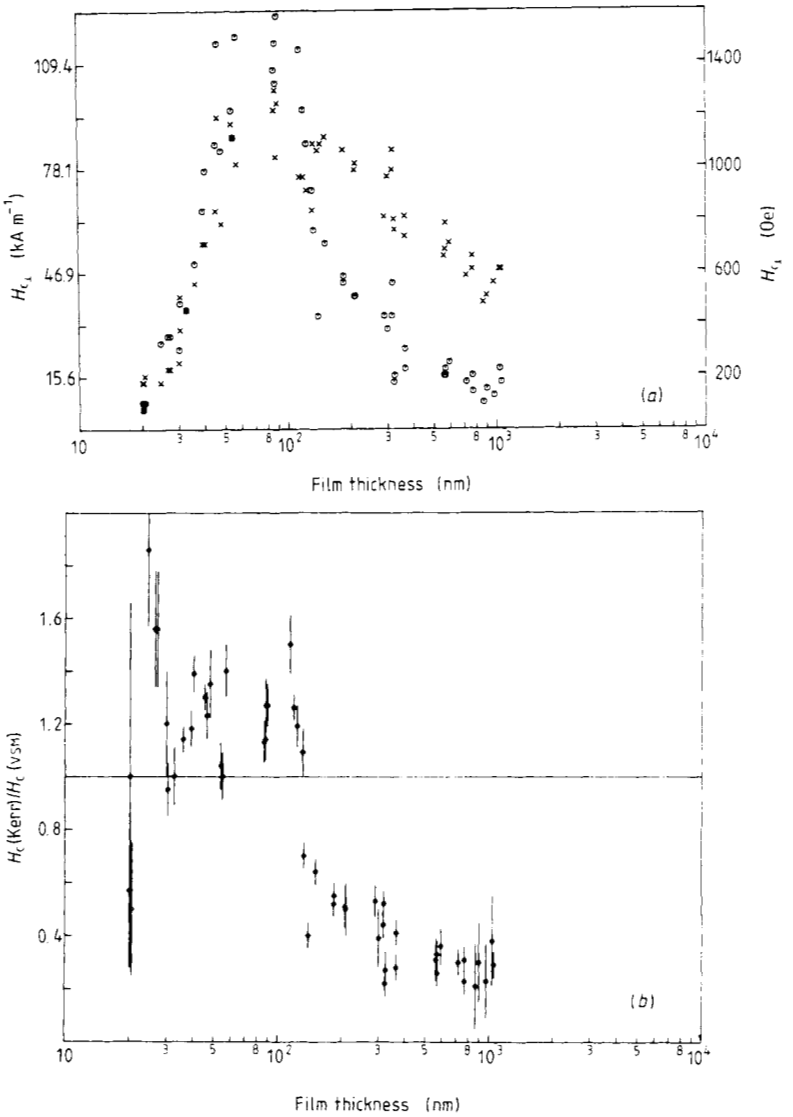

Figure 3. (*a*) Kerr (⊙) and VSM (×) coercivity versus film thickness for RF-sputtered CoCr (81/19 at.%). (*b*) Kerr/VSM coercivity ratio versus film thickness for RF-sputtered CoCr (81/19 at.%).

ratio smaller than 1. However it should be noted that the relative accuracy is lower here because of the low absolute values of both coercivities (see figure 4, part A). In part B of figure 4 the VSM and Kerr curves both reveal the so-called shoulder, which is characteristic for a well oriented uniaxial material like CoCr. Part C is an example of a large coercivity film, and in part D the result of a thicker film (363 nm) is shown, which may be regarded as typical for a practical recording film (≈500 nm). It is clear that the Kerr curve follows the shoulder of the VSM curve but decreases more rapidly to a lower remnant magnetisation and a lower coercivity at increasing opposite field strength. These two quantities (M_r and H_c) are strongly related, in fact for thicker films they are about equal (Wielinga *et al* 1982).

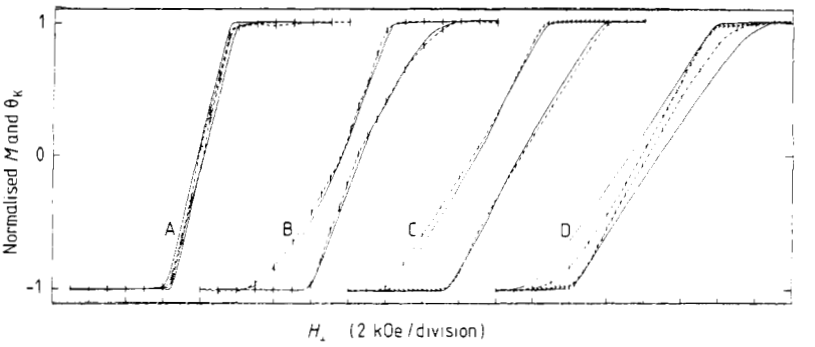

Figure 4. Normalised Kerr (----) and VSM (——) hysteresis curves of four RF-sputtered CoCr (81/19 at.%) samples with different film thickness: A, 20 nm; B, 33 nm; C, 54 nm; D, 363 nm. 2 kOe/division ≈ 160 kA m^{-1}/division.

4.2.2. Magnetron-sputtered CoCr81/19 at.%. The properties of magnetron films appear to be quite different to those of RF-sputtered films. The VSM coercivity slowly increases with the film thickness to reach a maximum of 90 kA m^{-1} (1100 Oe) at $t = 1.2$ μm (see figure 5(*a*)). The Kerr coercivity more or less follows the same curve which can also be seen from the ratio between both coercivities (figure 5(*b*)). In the case of most samples the Kerr coercivity is higher. Only four thin and four thick samples have a ratio smaller than one. Again, it should be noted that relative errors increase with a smaller film thickness. Analogous with RF films the expected discontinuity in the Kerr/VSM might be found at $t = 2.0$ μm. To clarify this, thicker films will be prepared. Illustrative examples are shown in figure 6, first that of an 80 nm thin film and then that of a thicker film ($t =$ 230 nm), which already shows the typical sheared rectangular form of the VSM curves which all thicker magnetron films possessed. Only the very thin films ($t < 100$ nm) showed a shoulder (and/or 'waistlining' near the origin). On the contrary most films thicker than about 1.1 μm exhibited a broadening in the Kerr hysteresis curve near the origin (see figure 6, part C). A thick film ($t = 1.9$ μm) without this broadening, and so with a Kerr/VSM coercivity ratio smaller than one, is shown in figure 6, part D.

5. Discussion and conclusion

A discussion about the magnetic behaviour of sputtered CoCr is complicated by the dependence of the characteristics on sputter parameters. This is illustrated by the fact that film composition, saturation magnetisation, x-ray rocking curves ($\Delta\theta_{50}$) and in plane remnant magnetisation ($S_{\parallel}$) are more or less the same for RF and magnetron films, but our magnetron films reach a maximum coercivity only at about 1 μm, while the maximum of RF films is found below 100 nm.

However, some properties concerning the columnar morphology, segregation of Cr (Ouchi and Iwasaki 1985), saturation magnetisation (Hong *et al* 1985) and anisotropy have been reasonably well established by different authors. The natural domain width and structure has been studied by Lorentz TEM (Grundy *et al* 1984) and by neutron depolarisation (Hemmes *et al* 1984, Kraan *et al* 1986).

From our magneto-optic observations and the quoted literature it is clear that the magnetic properties at the surface differ from those in the bulk of the CoCr films. As a

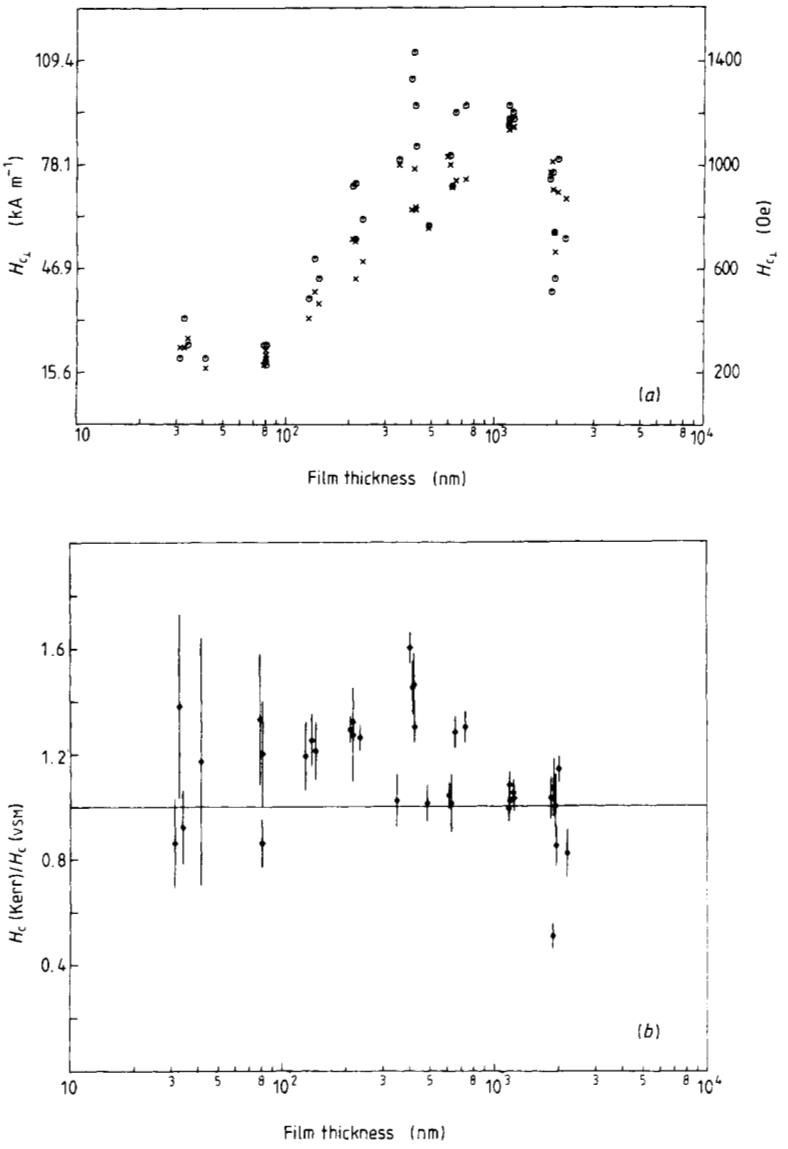

Figure 5. (*a*) Kerr (⊙) and VSM (×) coercivity versus film thickness for magnetron-sputtered CoCr (81/19 at.%). (*b*) Kerr/VSM coercivity ratio versus film thickness for magnetron-sputtered CoCr (81/19 at.%).

consequence the magnetisation cannot be homogeneous throughout the film during all stages of the hysteresis curve. The coercivity of the initial layer at the substrate side is found to be lower than 16 kA m^{-1} (200 Oe), regardless of film thickness. This is verified by Kerr measurements on the substrate side of CoCr sputtered on glass, as also reported by Smits *et al* (1984).

In explaining the dependence of coercivity on film thickness one has to assume a reversal mechanism, which is not necessarily the same for all film thicknesses. We will

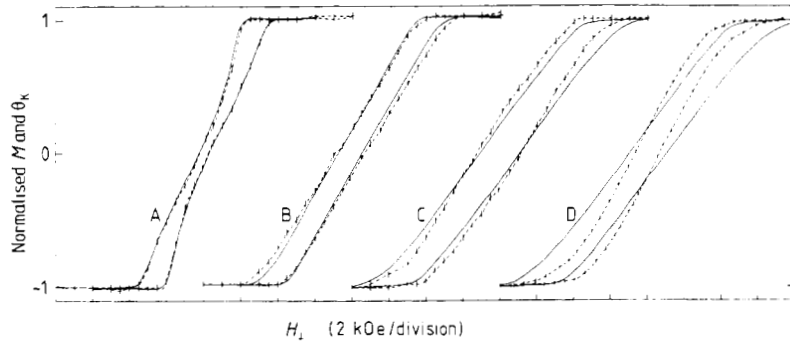

Figure 6. Normalised Kerr (----) and VSM (——) hysteresis curves of four magnetron-sputtered CoCr (81/19 at.%) samples with different film thickness: A, 80 nm; B, 233 nm; C, 1.23 μm; D, 1.88 μm. 2 kOe/division $\simeq$ 160 kA m^{-1}/division.

consider here the magnetic reversal with an external field perpendicular to the surface. Mainly, two models are proposed for the magnetic behaviour of CoCr; the particulate and the continuous model. Since both models cannot explain the magneto-optic results reported here and those in literature, a third intermediate model will be proposed.

The present results are discussed in the context of these models. Within the particulate model each column is considered as a single-domain particle exhibiting only magnetostatic interaction with all other columns. No exchange force exists across the boundaries because of the high concentration of chromium and/or oxygen in this region. The rotation of spins in each particle can either take place by coherent or incoherent rotation (buckling, curling or fanning). Coherent rotation is unlikely because it predicts much higher coercivities than those experimentally found. Besides, as mentioned above, the average magnetisation cannot be homogeneous throughout the film thickness. In the case of incoherent rotation it can be imagined that the vertical component of the spins at the surface in the remnant state is lower than that in the bulk because of demagnetising effects. This could explain the lower remnant magnetisation at the surface found for films with $t > t_c$, but it cannot explain at the same time that this value is higher than in the bulk for films with $t < t_c$.

In the continuous model we are faced with the same problem. In this model the reversal mechanism is thought to be the displacement of vertical (Bloch) domain walls more or less hindered by the column boundaries. Here spin directions at the surface may also deviate from the energetically favourable film normal due to demagnetisation, but this is not consistent with the behaviour of films with $t < t_c$.

In a third model the formation of reversed domains (spikes) within the main domains at the surface is proposed. The existence of in-plane or reversed closure domains in CoCr was earlier proposed by Smits *et al* (1984) to explain their results analogous to the results reported here. In their reports on neutron-depolarisation experiments Kraan *et al* (1985) and Hemmes *et al* (1985) also proposed the existence of spike domains. In his review on coercivity mechanisms Livingston (1981) concluded that for materials based on crystal anisotropy magnetisation reversal occurs by nucleation and growth of reversed domains.

A theoretical support for reversed domains in uniaxial thin films with the easy axis perpendicular to the surface, as in CoCr, is provided by Privorotskii (1976) and more recently by Hubert (1985) who applied his theory to CoCr. Partly based on the pub-

lication of Smits *et al* (1984) the following division in overlapping regions can be made:

Region 1, $t = 0$–30 nm. Both coercivities and hysteresis curves are about equal here because the penetration depth of light is sufficient to explore the whole film thickness (see figure 4, parts A and B). The coercivity is low because the initial layer has a low coercivity.

Region 2, $t = 30$ nm–t_c. The Kerr coercivity is larger here because the low coercivity of the initial layer now only lowers the VSM value. Both coercivities reach a maximum in this region. The sudden drop in the Kerr coercivity can be explained by the formation of spikes at the air surface. A minimum film thickness is needed before spikes are energetically favourable. Using the Privorotskii model a critical thickness of about 50 nm can be calculated assuming a domain wall width of 10 nm. This is still in the order of the t_c of 125 nm we found for RF films but cannot explain the magnetron results.

Formation of spikes at the substrate side is also quite possible with the boundaries of the small crystals acting as nucleation points for the spikes and providing regions of low domain wall energy. This helps to lower the VSM coercivity.

Region 3, $t > t_c$. Here the Kerr coercivity further decreases with increasing film thickness. The VSM coercivity also decreases but remains higher than the Kerr value. Further branching of the (spike) domain structure could well explain the lowering of both coercivities with increasing thickness.

Because coercivity, domain structure and reversal mechanism in thin films are closely related the latter also has to be discussed in the context of the third model. If reversed domains do exist in CoCr the most likely reversal mechanism is the one in which the reversed domains grow at the expense of the main one. The reversed domains would also disturb any tendency to buckling, fanning or any other type of particle reversal mechanism.

With respect to films having a thickness $t < t_c$ (or $H_{c\,\mathrm{Kerr}} > H_{c\,\mathrm{VSM}}$) one of the first two models would still apply. This last remark is of special interest to magnetron films, since these films with a thickness of about 500 nm, suitable for practical recording, do have a larger surface coercivity compared with the bulk value.

Further research on magnetron films, also extended to include larger film thicknesses is needed to clarify the deviating behaviour compared with RF films. Rotational hysteresis torque measurements could possibly reveal different reversal mechanisms for RF and magnetron films depending on film thickness.

Concluding it can be stated that:

(i) The rotating-analyser method is suitable for measuring the small Kerr rotation of ferromagnetic samples, thus obtaining information about the surface magnetic behaviour. Using a laser and a multiple reflection sample holder an accuracy of 0.002 deg could be obtained.

(ii) Comparing surface and bulk coercivity of sputtered-CoCr films a critical thickness is found (at least for the RF films) above which the Kerr/VSM coercivity ratio is smaller and below which it is larger than one. These results support the model of a branched domain structure of reversed domains within the main ones.

Acknowledgments

The authors would like to thank J D Baxter, F R Blom, G E van Dorssen, L Dubbeldam, J Span and K O van der Werff for their contribution to this work.

References

Abe M, Shono K, Kobayashi K, Gomi M and Nomura S 1982 *Japan. J. Appl. Phys.* **21** L22–4
Grundy P J, Ali M and Faunce C A 1984 *IEEE Trans. Magn.* **MAG-20** 794–6
Hanekamp L J, Lisowski W and Bootsma G A 1982 *Surf. Sci.* **118** 1–18
Hemmes K, Lodder J C, Rekveldt M Th and Kraan W H 1984 *J. Phys. D: Appl. Phys.* **17** L157–62
—— 1985 *Proc. ICMFS (Ansilomar, USA) 1985*
Hong M, van Dover R B, Bacon D B, Nakahara S, Gyorgy E M and van der Berg J M 1985 *ICM (San Francisco) 1985* paper 4D5
Hubert A 1985 *IEEE Trans. Magn.* **MAG-21** 1604–6
Iwasaki S 1980 *IEEE Trans. Magn.* **MAG-16** 71–6
Kraan W H, Rekveldt M Th, Hemmes K and Lodder J C 1986 *Int. Conf. on Neutron Scattering (Santa Fe) 1985*
Livingston J D 1981 *J. Appl. Phys.* **52** 2544–8
Lodder J C and Wielinga T 1984 *IEEE Trans. Magn.* **MAG-20** 57–9
Lodder J C, Wielinga T and Worst J 1983 *Thin Solid Films* **101** 61–81
Ouchi K and Iwasaki S 1985 *J. Appl. Phys.* **57** 4013–5
Privorotskii I 1976 *Thermodynamic Theorie of Domain Structures* (New York: Wiley)
Smits J W, Luitjens S B and Geuskens R W J 1984 *IEEE Trans. Magn.* **MAG-20** 60–2
Tsutsumi K, Fujii Y, Komori M, Numata T and Sakurai Y 1983 *IEEE Trans. Magn.* **MAG-19** 1760–2
Wielinga T, Lodder J C and Worst J 1982 *IEEE Trans. Magn.* **MAG-18** 1107–9